ORIGINAL ARTICLE

# Macrophages Are Involved in Gut Bacterial Translocation and Reversed by *Lactobacillus* in Experimental Uremia

Lingshuang Sun[1] · Hua Liu[2] · Hongli Jiang[2] · Meng Wei[2] · Shanshan Liang[1] ·
Meng Wang[2] · Kehui Shi[2] · Quan He[2]

**Abstract**

*Background* Uremia causes gut microbiome dysbiosis, which is characterized by a reduction in beneficial bacteria. Intestinal bacterial translocation (BT) contributes to microinflammation in uremia, which is associated with adverse outcomes. Whether macrophages are involved in BT remains unclear.

*Aims* We investigated the involvement of macrophages in BT and microinflammation in uremic rats and whether *Lactobacillus LB* can influence macrophage activity.

*Methods* Male Sprague–Dawley rats were randomly divided into three groups: sham, uremia, and uremia + probiotic. Macrophages and GFP-labeled tracer bacteria in intestinal and extraintestinal tissues were observed by fluorescence microscopy. The macrophage ultrastructure was examined by transmission electron microscopy. Immunochemistry was used to analyze the expression of cluster of differentiation 11a (CD11a), inducible nitric oxide synthase (iNOS), and intercellular adhesion molecule-1 (ICAM-1). RT-PCR and Western blot were employed to assess the mRNA and protein expression of early growth response gene 1 (EGR1) and toll-like receptor 4 (TLR4).

*Results* In uremic rats, the colocalization of GFP-labeled tracer bacteria and macrophages was visible in intestinal and extraintestinal tissues. Compared with the sham group, the uremic macrophages showed fewer cytoplasmic protrusions and pseudopodia. Administration of *Lactobacillus LB* restored the protrusions and pseudopodia. Compared with the sham group, the uremia group exhibited macrophages with higher staining intensities for CD11a, iNOS, and ICAM-1, and higher mRNA and protein expression of TLR4 and EGR1.

*Conclusions* Intestinal macrophages in the uremic rats are polarized toward a proinflammatory phenotype, resulting in microinflammation. Macrophages with impaired phagocytic function are associated with BT. *Lactobacillus LB* reduces BT by enhancing macrophage phagocytosis.

**Keywords** Macrophages · Bacterial translocation · Microinflammation · Uremia · Probiotics

## Introduction

Microinflammation is a common feature of end-stage renal disease, which is associated with adverse patient outcomes [1]. Research suggests that translocation of bacteria and endotoxins from the gut to the blood may be the cause of microinflammation [2]. Our previous research indirectly demonstrated the occurrence of intestinal bacterial translocation (BT) in a uremic rat model, as evidenced by an increased density of the green fluorescent protein (GFP)-labeled tracer bacterial gene [3] and by detection of intestinal bacterial genomic DNA in extraintestinal tissues [4]. However, direct evidence for BT in uremia is limited.

Macrophages with the M1 (proinflammatory) phenotype play a critical role in the progression of a number of kidney diseases [5] and act as critical effector cells in the initiation of inflammation in the pathogenesis of metabolic diseases

✉ Hongli Jiang
  j92106@sina.com

1  School of Medicine, Xi'an Jiaotong University, Xi'an, Shaanxi, China

2  Dialysis Department of Nephrology Hospital, First Affiliated Hospital of Medicine School, Xi'an Jiaotong University, Xi'an 710061, Shaanxi, China

[6]. The uptake of enterohemorrhagic *Escherichia coli* by M cells and underlying macrophages in the Peyer's patches may be a critical step in BT and is related to the efficiency of the infection [7]. The lipopolysaccharide (LPS) components of bacteria, a ligand of toll-like receptor 4 (TLR4), are expressed on various immune cells, including macrophages. TLR4 is a mediator of atherosclerosis, which may imply that increased LPS/TLR4 signaling could be a driving factor in the accelerated atherogenesis of chronic kidney disease patients [8]. LPS also induces activation of the early growth response gene 1(EGR1) on macrophages, and the LPS-induced expression of tumor necrosis factor-α (TNF-α) is directly mediated through the transcription factors EGR1 and nuclear factor-κB [9]. Hence, bacterial products may activate macrophages and other immune cells to produce proinflammatory mediators and trigger inflammation [10]. However, the involvement of intestinal macrophages in the uremic state is still unknown.

Our previous study has shown that uremic rats develop gut microbiome dysbiosis, which is characterized by a reduction in beneficial bacteria (*Bifidobacteria* and *Lactobacilli*) and increased numbers of pathogenic and opportunistic pathogens [11]. So, we considered that probiotic supplementation that reduces the uremic state may have beneficial effects. As expected, *Bifidobacteria* alleviate BT and ameliorate microinflammation in experimental uremia [3]. In addition, *Lactobacilli* play a significant role in maintaining the intestinal barrier function, improving local intestinal immunity, and enhancing antagonism toward pathogens [12, 13] as well as reducing mucosal dysbiosis [14]. However, it is still not clear whether *Lactobacilli* prevent BT and decrease microinflammation in uremic rats.

Therefore, we designed an experiment to observe the colocalization of bacteria and macrophages by GFP-labeled tracer bacteria in extraintestinal tissues and to reveal the role of intestinal macrophages in BT in uremic rats. Moreover, an index that represents the function of intestinal macrophages would be helpful in understanding the involvement of macrophages in microinflammation. In view of the imbalance of the intestinal microbiome in uremic rats and the beneficial effect of *Lactobacilli* on the intestinal epithelial barrier function, the aim of the present study was to investigate the effect of *Lactobacillus LB* by evaluating BT, macrophage function, and microinflammation in uremic rats.

## Materials and Methods

### Tracer Bacteria

GFP-labeled tracer bacteria were constituted by transforming competent *E. coli* DH5 cells with the recombinant plasmid-enhanced GFP (Clontech Laboratories, Palo Alto, CA, USA) into competent *E. coli* DH5α cells. Transformed *E. coli* DH5α clones were inoculated into Luria–Bertani broth containing 100 mg/L ampicillin and incubated overnight at 37 °C. The concentration of transformed GFP-labeled *E. coli* DH5α bacteria was adjusted to $10^8$ CFU/mL.

### Animals

A total of 55 Sprague–Dawley rats (200–220 g) underwent a total 5/6 nephrectomy. The rats underwent excision of approximately two-thirds of the left renal cortical mass; 1 week later, the whole right kidney was removed. Meanwhile, 20 rats in the sham group underwent two surgical procedures at the same time, without loss of renal mass but only an open renal capsule. Ten weeks after the total 5/6 nephrectomy, 15 uremic rats had died, so 40 uremic rats and 20 sham-operated rats (sham group) were available for study. The uremic rats were assigned randomly to two groups: uremia ($n = 20$) and uremia + probiotic ($n = 20$). The rats in the uremia + probiotic group received *Lactobacillus LB* (Lacteol, Fort, France) (1 mL, $10^9$ CFU/mL) by gavage every day for 4 weeks. Research was conducted in accordance with the criteria outlined in the Guide for the Care and Use of Laboratory Animals. The research proposal was approved by the Animal Research Committee of the First Affiliated Hospital, School of Medicine, Xi'an Jiaotong University.

Ten rats in each group were randomly selected to receive 1 mL of the suspension of GFP-labeled tracer bacteria intragastrically at 2 h before anesthesia for immunofluorescence and transmission electron microscopy analyses. The remaining 10 rats in each group that did not receive the GFP-labeled tracer bacteria were euthanized for immunohistochemistry, reverse transcription polymerase chain reaction (RT-PCR), and Western blot analyses. Rat body weights were obtained before killing. Small segments of the upper jejunum (5 cm below the angle of Treitz), terminal ileum (5 cm above the ileocecal valve), transverse colon (5 cm below the ileocecal valve), mesenteric lymph nodes (MLNs), liver, and spleen were excised for analysis.

### BT Studies

For immunofluorescence microscopy, samples were embedded in Tissue-Tek O.C.T. and stored at −20 °C. Frozen section (5 μm in thickness) were prepared and incubated with 0.1 % trypsin (Difco Laboratories, Detroit, MI, USA) in phosphate-buffered saline at 37 °C for 30 min to expose the antigens, blocked with normal goat serum for 1 h, incubated with 1:200 mouse anti-rat-CD68 antibody or 1:200 rabbit anti-GFP antibody (both from Abcam,

Cambridge, MA, USA), and then incubated for 2 h with 1:1000 anti-mouse-Dylight 633 IgG and 1:1000 anti-rabbit-FITC IgG (both from CWBio, Wuhan, China).

For analysis by transmission electron microscopy, small tissue pieces were fixed in 2.5 % glutaraldehyde solution in 0.15 M phosphate buffer at pH 7.2. Specimens were post-fixed in 1 % osmium tetroxide dissolved in saline and impregnated overnight in an aqueous solution of 1 % uranyl acetate. Specimens were embedded in polyester resin, and ultrathin sections of the embedded specimens were made. Sections were stained with lead citrate and uranyl acetate and viewed with anH-7650 electron microscope (Hitachi, Tokyo, Japan).

## Real-Time PCR Analysis of EGR1 and TLR4 Gene Expression

Total RNA was isolated using an Ultrapure RNA Kit (CWbio, Beijing, China). The primers were designed and synthesized by Samgon Biotechnology Company (Shanghai, China). The primer sequences were as follows: *EGR1*: forward: 5′-AGCCTTCGCT CACTCCACTA-3′, reverse: 5′-GACTCAACAG GGCAAGCATA C-3′; *TLR4*: forward: 5′-TGGCATCATC TTCATTGTCC-3′, reverse: 5′-CAGAGCATTG TCCTCCCACT-3′. PCR was performed using the real-time PCR system (SLAN, Shanghai, China), which was used with the Fast Start Universal SYBR Green Master (Roche, Basel, Switzerland). The PCR conditions were as follows: predenaturation at 95 °C for 10 min, followed by 40 cycles of denaturation at 95 °C for 15 s and annealing/extension at 60 °C for 60 s. The jejunum of the sham group was set as 1. Fold changes were calculated by the $2^{-\Delta\Delta C_t}$ method.

## Western Blotting of EGR1 and TLR4 Proteins

Protein concentrations were determined using a BCA protein assay kit (CWbio, Beijing, China). Equal amounts of protein samples were loaded, separated using 6 or 8 % SDS-PAGE, and transferred to immunoblot polyvinylidene difluoride membranes (Bio-Rad Laboratories, Inc, Hercules, CA, USA) by electroblotting. Immunoblotting was performed with 1:800 anti-EGR1, 1:800 anti-TLR4 (both from Abcam), and 1:1000 anti-β-actin (CWbio, Beijing, China). Immunoblots were then exposed to secondary horseradish peroxidase (HRP)-conjugated anti-mouse IgG (1:3000) or anti-rabbit IgG (1:3000) (both from Boster) and visualized using a chemiluminescent HRP substrate kit (Millipore, Billerica, MA, USA). Image analyses were performed using the AlphaEaseFC software package (version 4.0, Alpha Innotech, San Leandro, CA, USA). The quantitative results were normalized to β-actin levels.

## Immunohistochemical Analyses

The samples were fixed in 4 % paraformaldehyde over 24 h, dehydrated in ethanol, cleared in xylene, embedded in paraffin blocks, and cut into 4- to 5-μm-thick sections. Sections were incubated with 1:50 anti-CD11a, 1:160 anti-inducible nitric oxide synthase (iNOS), and 1:50 anti-intercellular adhesion molecule-1 (ICAM-1) antibodies (all from Abcam) and then with anti-mouse or anti-rabbit IgG-HRP secondary antibodies (Boster, Wuhan, China). The color was developed by using the DAB Horseradish Peroxidase Color Development Kit (Boster, Wuhan, China). Antigens were retrieved by the microwave method.

All sections were reviewed independently by two observers who recorded the histopathological characteristics and specific immunoreactivity (IR). The intensity of the immunoreactivity was stratified into four categories: 0 (−IR, non-staining), 1 (+IR, faint yellow), 2 (++IR, sandy beige), and 3 (+++IR, brown). The area of staining was classified into four groups: 1 (0–5 % of the cells exhibit IR), 2 (6–25 % exhibit IR), 3 (26–50 % exhibit IR), and 4 (>50 % exhibit IR). The staining index was calculated by multiplying the area by the intensity and was classified as follows: weak (0–2), moderate (3–4), and strong (>6).

## Blood Analyses

Creatinine, urea nitrogen, endotoxin (LPS), C-reactive protein (CRP), interleukin (IL)-6, TNF-α, and hematocrit in the abdominal aorta blood of 10 randomly selected rats from each group were assessed.

## Statistical Analyses

All statistical analyses were performed using the IBM SPSS 19.0 software package (SPSS Inc, Chicago, IL, USA). Quantitative data are reported as the mean ± standard deviation (SD). The Student's *t* test was used to compare continuous variables, whereas the Chi-squared or Fisher's exact test was used to compare categorical variables. Differences with $p < 0.05$ were considered statistically significant.

## Results

### General Data, Endotoxin Levels, and Plasma Inflammatory Biomarkers

The blood biochemical analyses are summarized in Table 1. As expected, the uremia and uremia + probiotic groups exhibited significantly higher mean serum creatinine and urea nitrogen concentrations, compared to the

**Table 1** Body weight, hematocrit, and blood chemistry results

| Group ($n = 10$) | Body weight (g) | Hematocrit (%) | Creatinine (μmol/L) | Urea (mmol/L) | Endotoxin (Eu/mL) | CRP (mg/mL) | IL-6 (pg/mL) | TNF-α (pg/mL) |
|---|---|---|---|---|---|---|---|---|
| Sham | 560.4 ± 16.6 | 58.25 ± 2.0 | 31.5 ± 6.7 | 6.05 ± 0.85 | 0.016 ± 0.005 | 2.48 ± 0.28 | 18.26 ± 3.72 | 20.9 ± 0.28 |
| Uremia | 516.6 ± 14.5* | 47.7 ± 3.0* | 95.7 ± 35.6* | 18.10 ± 8.50* | 0.033 ± 0.009* | 5.2 ± 0.77* | 31.07 ± 10.06* | 30.4 ± 7.73* |
| Uremia + probiotic | 529.4 ± 20.9* | 50.4 ± 3.0* | 87.8 ± 33.6* | 18.56 ± 8.32* | 0.021 ± 0.007** | 3.22 ± 1.12** | 19.45 ± 5.22** | 21.5 ± 4.38** |

Data are presented as the mean ± SD

* $p < 0.05$ versus the sham group

** $p < 0.05$ versus the uremia group

sham group. The plasma levels of endotoxin, CRP, IL-6, and TNF-α in the uremia group were greater than those in the sham group ($p < 0.05$). Fortunately, after treatment with probiotic, these indices became lower, compared to the group without probiotic treatment ($p < 0.05$).

## BT in Uremic Rats

GFP-labeled tracer bacteria exhibited a green fluorescent signal in the ileum (Fig. 1d), MLNs (Fig. 2a), liver (Fig. 2d), and spleen (Fig. 2g) of rats in the uremia group. The macrophage marker CD68 showed red fluorescence in the ileum (Fig. 1e), MLNs (Fig. 2b), liver (Fig. 2e), and spleen (Fig. 2h). Colocalization of the macrophage marker CD68 and GFP-labeled tracer bacteria of rats in the uremia group indicated that these bacteria were within the macrophages (Figs. 1f, 2c, f, i), while the merge of the two images gave a yellow fluorescent signal.
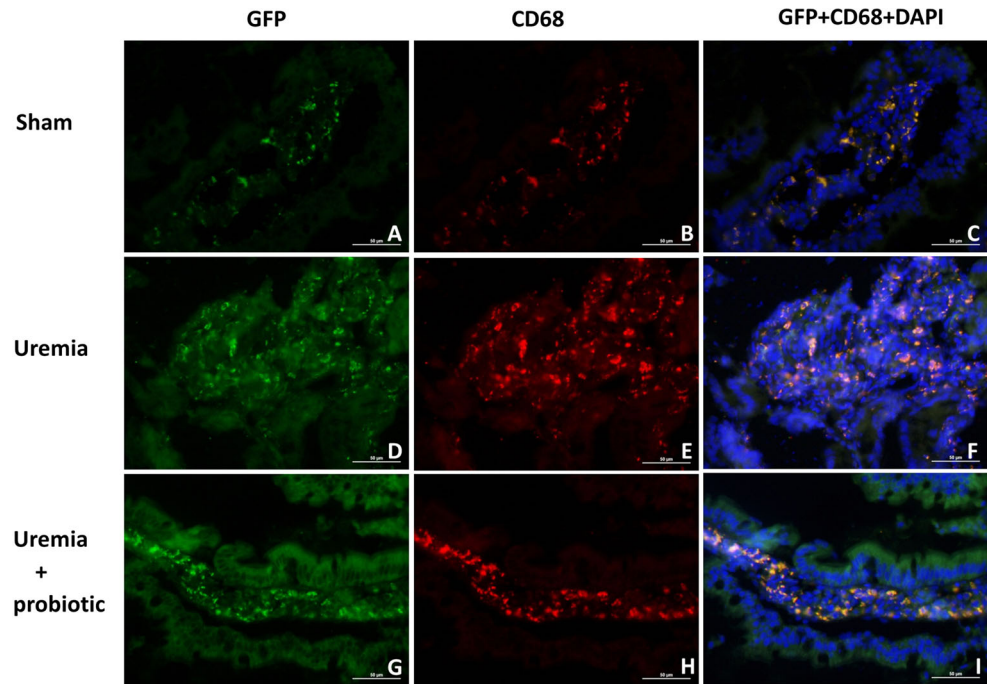
The green fluorescent signal for bacteria (Fig. 1a) and red fluorescence for the macrophage marker CD68 (Fig. 1b) were rare in the ileum in the sham group. Meanwhile, macrophages and GFP-labeled tracer bacteria in the ileum of rats in the uremia + probiotic group were colocalized (Fig. 1g–i).

## Morphology of the Intestinal Mucosa and Macrophages in Uremia

Compared to the sham group (Fig. 3a–c), the intestinal mucosa in the uremia group exhibited small and irregular microvilli, lightly stained tight junctions, and obscure desmosome junctions between epithelial cells; in addition, more vacuolated mitochondria appeared in the uremia group (Fig. 3c, f, i). Compared to the uremia group, the intestine in the uremia + probiotic group exhibited restoration of the mucosal microarchitecture, with increased microvilli and better organization of the epithelial layer (Fig. 3g–i). In the uremia group, tracer bacteria were adherent to and even transferred into the intestinal mucosa (Fig. 3e, f).

Compared to the sham group, intestinal macrophages of uremic rats showed fewer cytoplasmic protrusions and pseudopodia, decreased electron density, and greater numbers of organelles (especially lysosomes) from ruptured macrophages in the intercellular space (Fig. 4d–f). Compared to the uremia group, intestinal macrophages in the uremia + probiotic group exhibited a more activated micromorphology, with increased cell size, greater numbers of cytoplasmic protrusions and pseudopodia, abundant rough endoplasmic reticula, and higher numbers of intracellular primary and secondary lysosomes (Fig. 4g–i).

**Fig. 1** Immunofluorescence of macrophages (CD68, red signal) together with the green fluorescence of GFP bacteria in the ileum. All sections were counterstained with DAPI (*blue*). **a, d, g** GFP, **b, e, h** CD68, **c, f, i** GFP + CD68 + DAPI, **a–c** sham group, **d–f** uremia group, **g–i** uremia + probiotic group. *Scale bar* 50 μm



**Fig. 2** Immunofluorescence of macrophages (CD68, red signal) together with the green fluorescence of GFP bacteria in the MLNs, liver, and spleen of the uremia group. All sections were counterstained with DAPI (*blue*). **a, d, g** GFP, **b, e, h** CD68, **c, f, i** GFP + CD68 + DAPI, **a–c** MLNs, **d–f** liver, and **g–i** spleen. *Scale bar* 50 μm
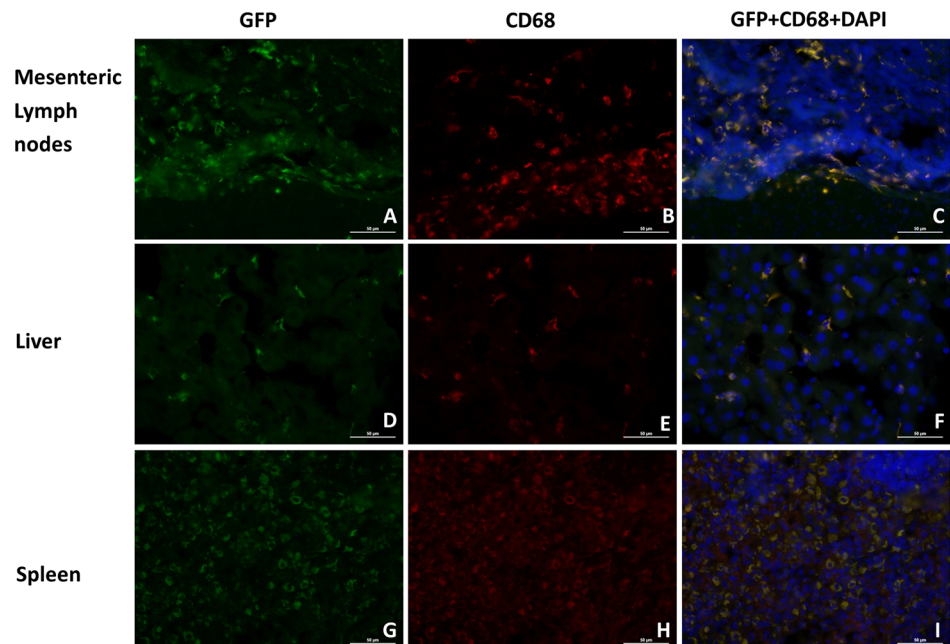


## Expression of EGR1 and TLR4

The fold change in *EGR1* and *TLR4* mRNA observed in the intestinal segments was significantly greater in the uremia group than in the sham group ($p < 0.05$ vs. the sham group jejunum; Fig. 5a). The fold change in *TLR4* mRNA among all intestinal segments of the uremia + probiotic group was significantly less than that in the uremia group ($p < 0.05$ vs. the corresponding intestinal segment of the uremia group; Fig. 5a).
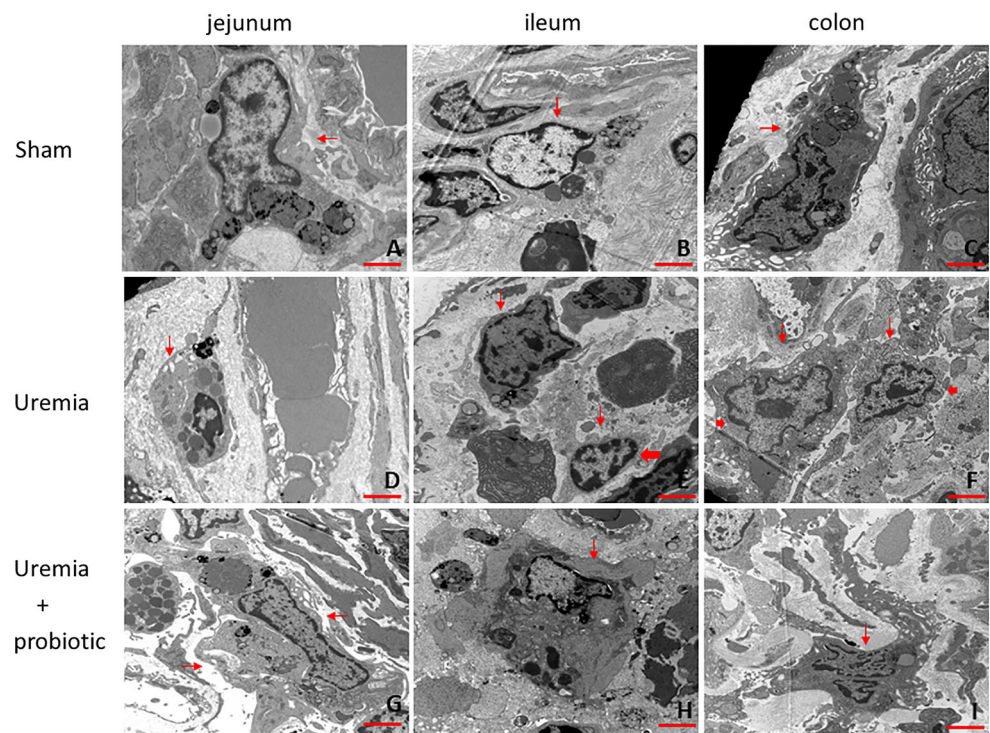
The expression levels of EGR1 and TLR4 protein in the intestinal segments were greater in the uremia group than in the sham group ($p < 0.05$ vs. the sham group jejunum; Fig. 5c). In addition, the levels of TLR4 protein in all intestinal segments of the uremia + probiotic group were significantly less than those in the uremia group ($p < 0.05$
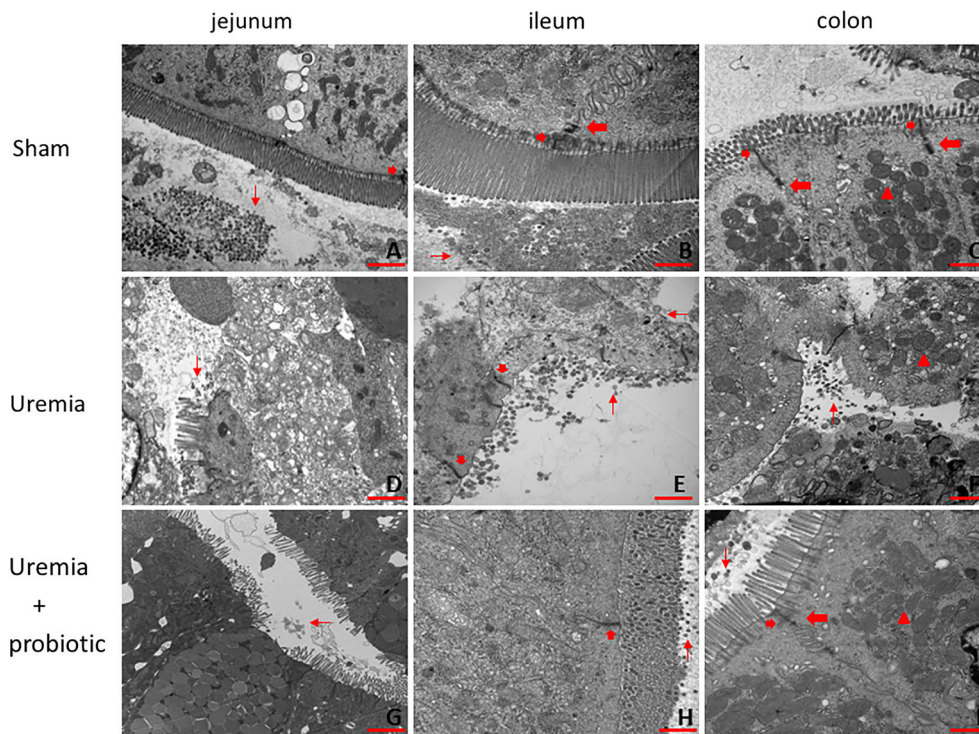
**Fig. 3** Transmission electron microscopy photomicrographs of the intestinal mucosa. **a**, **d**, **g** Jejunum, **b**, **e**, **h** ileum, **c**, **f**, **i** colon, **a–c** sham group, **d–f** uremia group, and **g–i** uremia + probiotic group. *Thin arrows* indicate tracer bacteria (**a–i**, except **c**). *Short thick arrows* indicate tight junctions (**a**, **b**, **c**, **e**, **h**, **i**). *Long thick arrows* indicate desmosome junctions (**b**, **c**, **i**). *Triangles* indicate mitochondria (**c**, **f**, **i**). *Scale bar* 2 μm (jejunum); 1 μm (ileum, colon)



**Fig. 4** Transmission electron microscopy photomicrographs of intestinal macrophages. **a**, **d**, **g** Jejunum, **b**, **e**, **h** ileum, **c**, **f**, **i** colon, **a–c** sham group, **d–f** uremia group, **g–i** uremia + probiotic group. *Thin arrows* indicate macrophages (**a–i**). *Long thick arrow* indicates a dying macrophage (**e**). *Short thick arrows* indicate decreases in macrophage electron density (**f**). *Scale bar* 2 μm
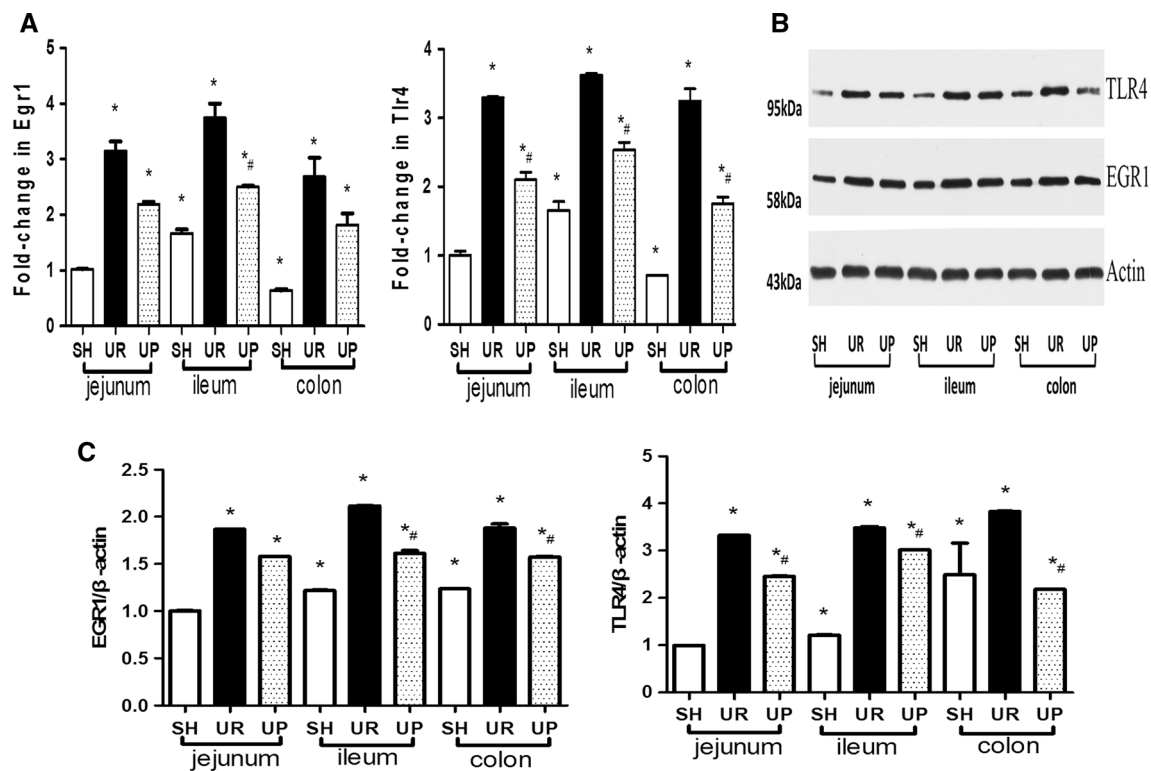
Fig. 5 Expression of EGR1 and TLR4. SH, sham group; UR uremia group, UP uremia + probiotic group. a Fold change in the gene expression levels of TLR4 and EGR1. b Immunoblots of EGR1 and TLR4 proteins. c Immunoblot band densities. In a, c, each column represents the mean ± SD of 10 replicates. *p < 0.05 compared to the sham group jejunum, and #p < 0.05 compared to the corresponding intestinal segment of the uremia group

vs. the corresponding intestinal segment of the uremia group; Fig. 5c).

## Expression of CD11a, iNOS, and ICAM-1

Compared to the sham group, all intestinal segments in the uremia group exhibited higher intensities of staining (+++) for CD11a and iNOS (Table 2). Staining was pronounced in the lamina propria and submucosa (Figs. 6a, 1b, d). All intestinal segments in the uremia + probiotic group stained positive for CD11a, and the staining distribution was the same as in the uremia group. Compared to the sham group, the colon and jejunum segments in the uremia group displayed a higher intensity of staining for ICAM-1, with staining being located primarily in the submucosa and lamina propria (Table 2; Fig. 6c).

## Discussion

In this study, we confirmed the existence of BT from the gut to extraintestinal tissues (MLNs, liver, and spleen) in a uremic rat by using GFP-labeled tracer bacteria. Intriguingly, macrophages and GFP-labeled tracer bacteria were colocalized, suggesting that macrophages loaded with bacteria cross the intestinal mucosa to promote BT in the uremic state. Intestinal macrophages have a strong tendency to polarize toward the M1 (proinflammatory) phenotype, which aggravates microinflammation. In addition, the phagocytic function was impaired in uremia. Treatment of uremic rats with Lactobacillus LB ameliorated microinflammation and BT by reducing the degree of intestinal macrophage activation and by improving macrophage phagocytic function, cytotoxicity, and local mucosal immunity.

We speculate that activation of intestinal macrophages assists BT and may play a carrier role in uremia. Intestinal bacteria can translocate across the abnormal intestinal barrier and contribute to the microinflammation present in patients with uremia [15]. The bacteria may cross the intestinal barrier through M cells or disrupted epithelial tight junctions [16]. We hypothesized that the uptake of bacteria by intestinal macrophages in the lamina propria caused edema and an eroded mucosa. The same finding was observed in macrophages by pathogenic bacteria [7]. Increased levels of endotoxin in the blood supplement the present data regarding the occurrence of BT in uremia and are beneficial to evaluate the extent of BT

**Table 2** Immunoreactivity of intestinal immune markers

| | Sham (n = 30) | | | Uremia (n = 30) | | | Uremia + probiotic (n = 30) | | |
|---|---|---|---|---|---|---|---|---|---|
| | Jejunum (n = 10) | Ileum (n = 10) | Colon (n = 10) | Jejunum (n = 10) | Ileum (n = 10) | Colon (n = 10) | Jejunum (n = 10) | Ileum (n = 10) | Colon (n = 10) |
| CD11a | −/1; 0 | +/1; 1 | −/1; 0 | +++/3; 9 | +++/2; 6 | +++/2; 6 | ++/2; 4 | ++/2; 4 | +++/1; 3 |
| iNOS | +/1; 1 | +/1; 1 | +/1; 1 | +++/2; 6 | +++/2; 6 | +++/2; 6 | ++/2; 4 | ++/2; 4 | ++/2; 4 |
| ICAM-1 | +/1; 1 | −/1; 0 | −/1; 0 | +++/1; 3 | ++/2; 4 | +++/2; 6 | ++/1; 2 | ++/2; 4 | ++/2; 4 |

Data are presented as staining intensity (−, +, ++, or +++)/staining area (1, 2, 3, or 4); staining index (0 to >6)
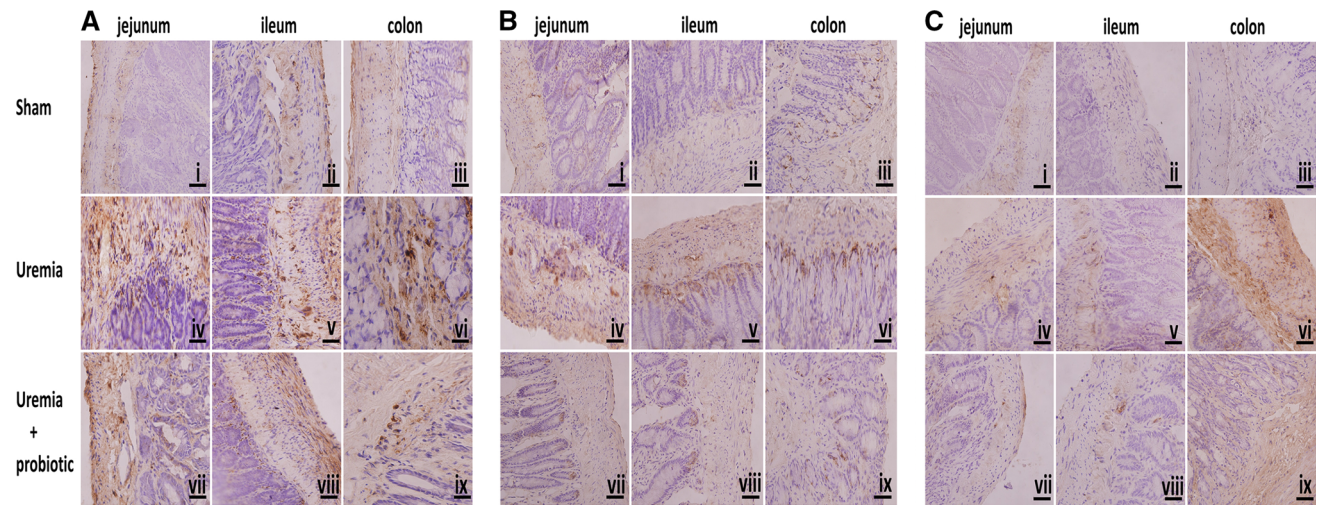


**Fig. 6** Photomicrographs showing immunoreactive staining of intestinal macrophage activation markers. (*i*, *iv*, *vii*) Jejunum, (*ii*, *v*, *viii*) ileum, (*iii*, *vi*, *ix*) colon, (*i–iii*) sham group, (*iv–vi*) uremia group, (*vii–ix*) uremia + probiotic group. *Scale bar* 50 μm. **a–c** Immunohistochemistry results for CD11a (**a**), iNOS (**b**), and ICAM-1 (**c**)

comprehensively. The results in the present research disclosed that macrophages and GFP-labeled tracer bacteria were colocalized. Intestinal macrophages can phagocytose the bacteria; however, due to overgrowth of intestinal bacteria and impaired phagocytic function of macrophages, the intestinal macrophages cannot destroy them in time to prevent BT. Intestinal bacteria that are not killed may cross the intestinal mucosa into the systemic circulation and extraintestinal tissues.

Previous research has revealed that intestinal macrophages are polarized toward the M1 phenotype when exposed to an abnormally high level of LPS [17]. Macrophages are activated by LPS via TLR4, yielding TNF-α. TNF-α induction in macrophages is at the transcriptional level [18]. Our data show that EGR1 mRNA was increased in intestinal tissue of the uremia group, which is consistent with the results of other investigators showing induction of EGR1 in macrophages stimulated by LPS [19]. CD11a, a subunit of integrin $\alpha_L\beta_2$, is important for macrophage migration/activation and is necessary for monocyte migration into the glomerulus and chronic glomerular injury [20]. CD11a regulates inflammation by recognition

and binding with ICAM-1 [21]. In other words, LPS activates TLR4 and EGR1, promoting the expression of CD11a and ICAM1 and eventually resulting in macrophage migration and activation, which release proinflammatory cytokines and costimulatory molecules. Activated macrophages also produce an iNOS-activated inflammatory response, which is known as classical activation. iNOS, together with the generation of nitric oxide and large quantities of proinflammatory cytokines (e.g., TNF-α and IL-6), is released when macrophages are activated by bacterial antigens, such as LPS [22]. This increased expression of proinflammatory markers was associated with elevated plasma levels of endotoxin, CRP, IL-6, and TNF-α. Under conditions of overgrowth of certain Gram-negative bacteria as well as disruption of the intestinal barrier in uremic animals, the bacteria were phagocytosed and transferred by macrophages, allowing endotoxins to enter into the circulation and to stimulate proinflammatory cytokines, leading to systemic inflammation under conditions of uremia [10, 23]. In this way, intestinal macrophages could contribute to the aggravation of microinflammation by allowing BT, which, in turn,

stimulates the systemic immune response and, ultimately, results in the development of complications commonly seen in uremic patients.

In the present research, *Lactobacillus LB* reduced BT and decreased the levels of macrophage activation markers, endotoxin, and proinflammatory cytokines. In addition, *Lactobacillus LB* restored the micromorphology of macrophages. Although the mechanisms underlying the reduction in BT by probiotics have not been fully elucidated, various hypotheses have been proposed. First, *Lactobacillus LB* induces an increase in the amount of beneficial bacteria and reduces the number of potentially pathogenic bacteria [24], which competitively prevent pathogens from adhering to and colonizing the intestinal mucosa. Second, *Lactobacillus LB* helps to maintain intestinal mucosal integrity by normalizing tight junction proteins [25]. Third, *Lactobacillus LB* is able to modulate non-specific cellular immune responses, improve intestinal macrophage phagocytic function, and reduce the degree of intestinal macrophage activation [26, 27]. *Lactobacillus casei* strain Shirota has been shown to improve kidney function and inflammation in hospitalized patients with acute gastroenteritis [28] as well as decrease blood urea concentrations in patients with chronic renal failure [29]. Moreover, *Lactobacillus* mutants cultured with the serum of uremic patients has been demonstrated to decompose uremic toxin [30]. These effects indicate that probiotics may be helpful to ameliorate the intestinal inflammatory response as well as to reverse intestinal macrophage activation and phagocytic function in uremia.

**Author contributions** LSS carried out the entire study protocol, participated in the immunohistochemical analysis, RT-PCR, and Western blot experiments, and drafted the manuscript. HL and MW participated in the immunofluorescence microscopy experiments. SSL and MW participated in the establishment of the animal model. KHS and QH participated in the study design and performed the statistical analysis. HLJ conceived of the study, participated in its design and coordination, and helped to draft the manuscript. All authors read and approved the final version of the manuscript.

**Compliance with ethical standards**

**Conflict of interest** The authors declare that they have no conflicts of interest.

**Ethics approval** All applicable international, national, and/or institutional guidelines for the care and use of animals were followed.

# Appendix

| Sample number | Gene name | | | The mean | | | $\Delta C_t = C_t$ (target gene) − $C_t$ (β-actin) | | $\Delta\Delta C_t = \Delta C_t$ (experimental) − $\Delta C_t$ (control) | | Fold change = $2^{-\Delta\Delta C_t}$ | |
|---|---|---|---|---|---|---|---|---|---|---|---|---|
| | β-actin | Tlr4 | Egr1 | β-actin | Tlr4 | Egr1 | Tlr4 | Egr1 | Tlr4 | Egr1 | Tlr4 | Egr1 |
| 1 | 16.32 | 24.38 | 26.71 | | | | | | | | | |
| 1 | 16.36 | 24.27 | 26.53 | 16.35 | 24.32 | 26.58 | 7.98 | 10.24 | 0.00 | 0.00 | 1.00 | 1.00 |
| 1 | 16.36 | 24.32 | 26.51 | | | | | | | | | |
| 2 | 16.68 | 23.02 | 25.25 | | | | | | | | | |
| 2 | 16.66 | 23.01 | 25.31 | 16.68 | 23.02 | 25.29 | 6.34 | 8.61 | −1.64 | −1.63 | 3.11 | 3.10 |
| 2 | 16.7 | 23.03 | 25.3 | | | | | | | | | |
| 3 | 15.26 | 22.11 | 24.5 | | | | | | | | | |
| 3 | 15.21 | 22.24 | 24.53 | 15.23 | 22.22 | 24.49 | 6.99 | 9.26 | −0.98 | −0.98 | 1.98 | 1.97 |
| 3 | 15.22 | 22.32 | 24.44 | | | | | | | | | |
| 4 | 16.12 | 23.68 | 26.02 | | | | | | | | | |
| 4 | 16.22 | 23.5 | 25.81 | 16.16 | 23.64 | 25.91 | 7.48 | 9.75 | −0.49 | −0.48 | 1.41 | 1.40 |
| 4 | 16.14 | 23.75 | 25.91 | | | | | | | | | |
| 5 | 16.18 | 22.37 | 24.64 | | | | | | | | | |
| 5 | 16.17 | 22.39 | 24.55 | 16.18 | 22.38 | 24.61 | 6.20 | 8.43 | −1.77 | −1.80 | 3.42 | 3.49 |
| 5 | 16.18 | 22.38 | 24.64 | | | | | | | | | |
| 6 | 14.62 | 21.53 | 23.71 | | | | | | | | | |
| 6 | 14.62 | 21.38 | 23.68 | 14.63 | 21.45 | 23.74 | 6.82 | 9.12 | −1.15 | −1.12 | 2.22 | 2.17 |
| 6 | 14.64 | 21.44 | 23.84 | | | | | | | | | |

| Sample number | Gene name | | | The mean | | | $\Delta C_t = C_t$ (target gene) $- C_t$ (β-actin) | | $\Delta\Delta C_t = \Delta C_t$ (experimental) $- \Delta C_t$ (control) | | Fold change $= 2^{-\Delta\Delta C_t}$ | |
|---|---|---|---|---|---|---|---|---|---|---|---|---|
| | β-actin | Tlr4 | Egr1 | β-actin | Tlr4 | Egr1 | Tlr4 | Egr1 | Tlr4 | Egr1 | Tlr4 | Egr1 |
| 7 | 15.76 | 24.33 | 26.69 | | | | | | | | | |
| 7 | 15.78 | 24.35 | 26.87 | 15.80 | 24.33 | 26.74 | 8.54 | 10.94 | 0.56 | 0.71 | 0.68 | 0.61 |
| 7 | 15.85 | 24.32 | 26.66 | | | | | | | | | |
| 8 | 15.07 | 21.52 | 24.02 | | | | | | | | | |
| 8 | 15.05 | 21.49 | 23.95 | 15.06 | 21.58 | 23.92 | 6.52 | 8.85 | −1.46 | −1.38 | 2.75 | 2.61 |
| 8 | 15.07 | 21.73 | 23.78 | | | | | | | | | |
| 9 | 15.5 | 22.76 | 25.21 | | | | | | | | | |
| 9 | 15.45 | 22.84 | 25.14 | 15.60 | 22.85 | 25.19 | 7.25 | 9.59 | −0.72 | −0.65 | 1.65 | 1.57 |
| 9 | 15.84 | 22.95 | 25.21 | | | | | | | | | |

# References

1. Schindler R. Causes and therapy of microinflammation in renal failure. *Nephrol Dial Transplant*. 2004;19:v34–v40.
2. Vaziri ND, Zhao Y-Y, Pahl MV. Altered intestinal microbial flora and impaired epithelial barrier structure and function in CKD: the nature, mechanisms, consequences and potential treatment. *Nephrol Dial Transplant*. 2015. doi:10.1093/ndt/gfv095.
3. Wei M, Wang Z, Liu H, et al. Probiotic Bifidobacterium animalis subsp. lactis Bi-07 alleviates bacterial translocation and ameliorates microinflammation in experimental uraemia. *Nephrology (Carlton)*. 2014;19:500–506.
4. Wang F, Zhang P, Jiang H, Cheng S. Gut bacterial translocation contributes to microinflammation in experimental uremia. *Dig Dis Sci*. 2012;57:2856–2862.
5. Zhou D, Huang C, Lin Z, et al. Macrophage polarization and function with emphasis on the evolving roles of coordinated regulation of cellular signaling pathways. *Cell Signal*. 2014;26:192–197.
6. Chawla A, Nguyen KD, Goh YS. Macrophage-mediated inflammation in metabolic disease. *Nat Rev Immunol*. 2011;11:738–749.
7. Chakravortty D, Etienne-Mesmin L, Chassaing B, et al. Interactions with M cells and macrophages as key steps in the pathogenesis of enterohemorragic *Escherichia coli* infections. *PLoS ONE*. 2011;6:e23594.
8. Kiechl S, Lorenz E, Reindl M, et al. Toll-like receptor 4 polymorphisms and atherogenesis. *N Engl J Med*. 2002;347:185–192.
9. Xu Z, Dziarski R, Wang Q, Swartz K, Sakamoto KM, Gupta D. Bacterial peptidoglycan-induced TNF-α transcription is mediated through the transcription factors Egr-1, Elk-1, and NF-κB. *J Immunol*. 2001;167:6975–6982.
10. Anders HJ, Andersen K, Stecher B. The intestinal microbiota, a leaky gut, and abnormal immunity in kidney disease. *Kidney Int*. 2013;83:1010–1016.
11. Wang F, Jiang H, Shi K, Ren Y, Zhang P, Cheng S. Gut bacterial translocation is associated with microinflammation in end-stage renal disease patients. *Nephrology (Carlton)*. 2012;17:733–738.
12. Servin AL. Antagonistic activities of lactobacilli and bifidobacteria against microbial pathogens. *FEMS Microbiol Rev*. 2004;28:405–440.
13. Delcenserie V, Martel D, Lamoureux M, Amiot J, Boutin Y, Roy D. Immunomodulatory effects of probiotics in the intestinal tract. *Curr Issues Mol Biol*. 2008;10:37.
14. Bujalance C, Jiménez-Valera M, Moreno E, Ruiz-López M-D, Lasserrot A, Ruiz-Bravo A. Lack of correlation between in vitro antibiosis and in vivo protection against enteropathogenic bacteria by probiotic lactobacilli. *Res Microbiol*. 2014;165:14–20.
15. Mafra D, Fouque D. Gut microbiota and inflammation in chronic kidney disease patients. *Clin Kidney J*. 2015;8:332–334.
16. Vaziri ND, Goshtasbi N, Yuan J, et al. Uremic plasma impairs barrier function and depletes the tight junction protein constituents of intestinal epithelium. *Am J Nephrol*. 2012;36:438.
17. Benoit M, Desnues B, Mege J-L. Macrophage polarization in bacterial infections. *J Immunol*. 2008;181:3733–3739.
18. Raabe T, Bukrinsky M, Currie RA. Relative contribution of transcription and translation to the induction of tumor necrosis factor-α by lipopolysaccharide. *J Biol Chem*. 1998;273:974–980.
19. Coleman D, Bartiss A, Sukhatme V, Liu J, Rupprecht H. Lipopolysaccharide induces Egr-1 mRNA and protein in murine peritoneal macrophages. *J Immunol*. 1992;149:3045–3051.
20. Kawasaki K, Yaoita E, Yamamoto T, Tamatani T, Miyasaka M, Kihara I. Antibodies against intercellular adhesion molecule-1 and lymphocyte function-associated antigen-1 prevent glomerular injury in rat experimental crescentic glomerulonephritis. *J Immunol*. 1993;150:1074–1083.
21. Marlin SD, Springer TA. Purified intercellular adhesion molecule-1 (ICAM-1) is a ligand for lymphocyte function-associated antigen 1 (LFA-1). *Cell*. 1987;51:813–819.
22. Bossola M, Sanguinetti M, Scribano D, et al. Circulating bacterial-derived DNA fragments and markers of inflammation in chronic hemodialysis patients. *Clin J Am Soc Nephrol*. 2009;4:379–385.
23. Shi K, Wang F, Jiang H, et al. Gut bacterial translocation may aggravate microinflammation in hemodialysis patients. *Dig Dis Sci*. 2014;59:2109–2117.
24. Jungersen M, Wind A, Johansen E, Christensen JE, Stuer-Lauridsen B, Eskesen D. The science behind the probiotic strain bifidobacterium animalis subsp. lactis BB-12®. *Microorganisms*. 2014;2:92–110.
25. Agostini S, Goubern M, Tondereau V, et al. A marketed fermented dairy product containing Bifidobacterium lactis CNCM I-2494 suppresses gut hypersensitivity and colonic barrier disruption induced by acute stress in rats. *Neurogastroenterol Motil*. 2012;24:376-e172.
26. Klein A, Friedrich U, Vogelsang H, Jahreis G. Lactobacillus acidophilus 74-2 and Bifidobacterium animalis subsp lactis DGCC 420 modulate unspecific cellular immune response in healthy adults. *Eur J Clin Nutr*. 2008;62:584–593.
27. Liévin-Le Moal V, Servin AL. Anti-infective activities of lactobacillus strains in the human intestinal microbiota: from probiotics to gastrointestinal anti-infectious biotherapeutic agents. *Clin Microbiol Rev*. 2014;27:167–199.

28. Akoglu B, Loytved A, Nuiding H, Zeuzem S, Faust D. Probiotic *Lactobacillus casei* Shirota improves kidney function, inflammation and bowel movements in hospitalized patients with acute gastroenteritis—a prospective study. *J Funct Foods*. 2015;17: 305–313.

29. Alatriste PVM, Arronte RU, Espinosa COG, Cuevas MDLÁE. Effect of probiotics on human blood urea levels in patients with chronic renal failure. *Nutr Hosp*. 2014;29:582–590.

30. Bai YH, Jiang YF, Jiang YS. *Lactobacillus bulgaricus* mutants decompose uremic toxins. *Ren Fail*. 2014;36:790–794.